applied sciences

MDPI

Article

Carbonate-Based Lanthanum Strontium Cobalt Ferrite (LSCF)–Samarium-Doped Ceria (SDC) Composite Cathode for Low-Temperature Solid Oxide Fuel Cells

Muhammed Ali S.A. [1], Jarot Raharjo [2], Mustafa Anwar [3], Deni Shidqi Khaerudini [4], Andanastuti Muchtar [1,5,*], Luca Spiridigliozzi [6,*] and Mahendra Rao Somalu [1]

1 Fuel Cell Institute, Universiti Kebangsaan Malaysia, UKM Bangi, Selangor 43600, Malaysia; mas@ukm.edu.my (M.A.S.A.); mahen@ukm.edu.my (M.R.S.)
2 Center of Materials Technology, Agency for the Assessment and Application of Technology (BPPT), Jl. M.H. Thamrin 8, Jakarta Pusat 10340, Indonesia; jarot.raharjo@bppt.go.id
3 U.S.-Pakistan Center for Advanced Studies in Energy, National University of Sciences and Technology, H-12, Islamabad 44000, Pakistan; mustafa@uspcase.nust.edu.pk
4 Research Center for Physics, Indonesian Institute of Sciences (LIPI), Gd.440-442, Kawasan Puspiptek Serpong, Tangerang Selatan, Banten 15314, Indonesia; deni.shidqi.khaerudini@lipi.go.id
5 Department of Mechanical and Manufacturing Engineering, Faculty of Engineering and Built Environment, Universiti Kebangsaan Malaysia, UKM Bangi, Selangor 43600, Malaysia
6 Department of Civil and Mechanical Engineering, University of Cassino and Southern Lazio, Via G. Di Biasio 43, 03043 Cassino (FR), Italy
* Correspondence: muchtar@ukm.edu.my (A.M.); l.spiridigliozzi@unicas.it (L.S.); Tel.: +60-389118379 (A.M.); Fax: +0389252699 (A.M.)

Received: 2 May 2020; Accepted: 26 May 2020; Published: 28 May 2020

Featured Application: Lanthanum strontium cobalt ferrite oxide (LSCF) based composite materials were used as a cathode for low temperature solid oxide fuel cells. Many studies have been reported in literature concerning their performance in improving the oxygen ion conducting behavior at temperatures below 600 °C. However, studies concerning the effect of samarium doped ceria–carbonate (SDCC) composite electrolyte content on the electronic network over the LSCF cathode surface are still limited. Therefore, the present study aims to fill the research gap with respect to SDCC content and its effect on the in-plane electronic conducting behavior at the surface of the LSCF cathode at low operating temperatures (i.e., 400–650 °C). Composite cathode was prepared by mixing LSCF cathode and SDCC composite electrolyte powders at different weight percentages (i.e., 70:30 wt %, 60:40 wt %, and 50:50 wt %) to determine the effect on the overall electrochemical performance under real fuel cell operating conditions.

Abstract: Perovskite-based composite cathodes, $La_{0.6}Sr_{0.4}Co_{0.2}Fe_{0.8}O_{3-\delta}$ (LSCF)–$Ce_{0.8}Sm_{0.2}O_{1.9}$-carbonate (SDCC), were investigated as cathode materials for low-temperature solid-oxide fuel cells. The LSCF was mixed with the SDC–carbonate (SDCC) composite electrolyte at different weight percentages (i.e., 30, 40, and 50 wt %) to prepare the LSCF–SDCC composite cathode. The effect of SDCC composite electrolyte content on the diffraction pattern, microstructure, specific surface area, and electrochemical performances of the LSCF–SDCC composite cathode were evaluated. The XRD pattern revealed that the SDCC phase diffraction peaks vary according to its increasing addition to the system. The introduction of SDCCs within the composite cathode did not change the LSCF phase structure and its specific surface area. However, the electrical performance of the realized cell drastically changed with the increase of the SDCC content in the LSCF microstructure. This drastic change can be ascribed to the poor in-plane electronic conduction at the surface of the LSCF cathode layer due to the presence of the insulating phase of SDC and molten carbonate. Among the cathodes investigated, LSCF–30SDCC showed the best cell performance, exhibiting a power density value of 60.3–75.4 mW/cm^2 at 600 °C to 650 °C.

Keywords: SOFC; perovskite; composites; cathode; electrical performance

1. Introduction

Solid oxide fuel cells (SOFCs) are the most promising electrochemical devices for the generation of clean energy in the near future [1]. However, they actually operate at high temperatures, i.e., between 700 and 1000 °C [2]. These high operating temperatures can cause very serious thermal and chemical instability issues at the electrolyte–electrode and sealant–interconnect interfaces, thus limiting their application [3–5]. Therefore, numerous researchers have focused their studies on reducing the operating temperature below 600 °C [6–8]. Low operating temperature SOFCs could minimize the durability and reliability issues, consequently increasing their life expectancy and range of application [9]. However, at reduced operating temperatures, the kinetics of thermally activated oxygen reduction reaction (ORR) at the cathode side were found to slow down the electrochemical reactions between the cells, and thereby contribute to high interfacial polarization resistance [10]. The functional requirements of a good cathode material must include high catalytic activity towards ORR, high electronic and ionic conductivity, adequate porosity (≈30%), and excellent thermal stability with the other cell components. Therefore, it is necessary to develop new cathode materials compatible with the other cell components and with high electrocatalytic activity towards ORR at low operating temperatures [11]. Perovskite oxide $La_{0.6}Sr_{0.4}Co_{0.2}Fe_{0.8}O_{3-\delta}$ (LSCF) is one of the most promising cathode materials due to its high conductivity and excellent electro-catalytic activity for ORR at intermediate temperatures (600–800 °C) [12]. Furthermore, LSCF also exhibits excellent chemical and thermal compatibility with doped ceria electrolytes such as samarium-doped ceria (SDC) and gadolinium–doped ceria (GDC) materials, which are both promising electrolyte materials at reduced operating temperatures [13–16]. However, LSCF cathode possesses severe microstructural and structural degradation at temperatures above 600 °C under fuel cell operating conditions [17]. To prevent or control the LSCF cathode degradation, researchers have adopted different strategies, such as surface enhancement treatment and nanostructured architecture [18,19].

Constructing the composite cathode by mixing LSCF with pure ionic conducting electrolyte material is an effective strategy for suppressing the compositional changes within the LSCF structure. However, the presence of pure ionic conducting materials, such as SDC electrolyte, could affect the electronic network at the surface of the LSCF cathode, thus causing significant decreases in the electronic conductivity of the LSCF cathode material itself [20]. This eventually increases the charge transfer resistance at the LSCF cathode during the fuel cell operation, consequently affecting the overall performance of the cell. This is because the electrochemical reactions at the LSCF cathode consists of two physicochemical processes: (1) charge transfer process associated with incorporation of O^{2-} ion at the cathode/electrolyte interface and electronic transfer at the interconnect/cathode interface, and (2) oxygen dissociation/adsorption on the cathode surface [21]. This electrochemical process at the cathode can be enhanced by introducing oxide ion conducting or superionic conducting materials to their microstructure. Many studies proved that the presence of eutectic carbonate salts ($(Li/Na/K)_2CO_3$) in the SOFC component backbone improved the overall performance of the fuel cell below 600 °C [22–26]. These carbonate based SOFC exhibited the highest cell performance, ranging from 300 mW/cm^2 to 1100 mW/cm^2 at 400 °C to 600 °C [27]. Therefore, the addition of carbonates to LSCF cathode material could improve its structural stability due to its melting characteristics at low temperatures.

LSCF based composite cathodes have been widely studied with SDC–carbonate (SDCC) electrolyte materials to improve its oxygen-ion conduction and structural stability at low operating temperatures. For instance, Rahman et al. reported single cell performance based on SDC–carbonate (SDCC) and LSCF composite cathode and found that the composite cathode exhibited power densities as high as 117.9 and 120.4 mW/cm^2 at an operation temperature of 550 °C [28]. In addition, Rahman et al. [29] also proposed that different powder mixtures of SDCC influenced the surface area and thermal expansion coefficient of the prepared composite cathode powder. However, studies on the effect of

SDCC composite electrolyte content on the electronic network over the LSCF cathode surface are still very limited. Therefore, this study aims to analyze the effect of SDCC composite electrolyte content on the in-plane electronic conducting behavior at the surface of the LSCF cathode at low operating temperatures (400–650 °C). The composite cathode is prepared by mixing LSCF with SDCC composite electrolytes at different weight percentages (i.e., 70:30 wt %, 60:40 wt %, and 50:50 wt %) to determine the effect on the overall electrochemical performance under real fuel cell operating conditions. The phase, microstructure, particle size distribution, BET specific surface area, and electrochemical performance of the LSCF–SDCC composite cathodes pellets were deeply analyzed in this study.

2. Experimental Procedure

2.1. Synthesis and Characterization of the Powder

The LSCF cathode and SDC electrolyte were prepared via glycine–nitrate and citric acid-assisted sol–gel processes, respectively. The detailed descriptions of the preparation procedures of LSCF cathode and SDC electrolyte powders are available in our previous publications [30,31]. The LSCF–SDCC composite cathode was realized by using the following procedure: Firstly, the SDCC composite electrolyte powder was prepared by mixing the prepared SDC powder and 30 wt % binary carbonates $Li_{1.34}Na_{0.66}CO_3$ via high-speed ball milling technique to prepare the SDCC composite electrolyte [32]. Secondly, the prepared SDCC composite electrolyte powder was mixed with the LSCF at different weight percentages. Finally, the resulting mixture was calcined at 680 °C for 1 h to obtain the desired LSCF–SDCC composite cathode powders. The weight percentages of the SDCC composite electrolyte content within the LSCF cathode varied from 30 wt % to 50 wt % in order to investigate the effect of SDCC content on the electrochemical performance of the LSCF–SDCC composite cathode. The prepared LSCF–SDCC composite cathode powders were labeled as LSCF–30SDCC, LSCF–40SDCC, and LSCF–50SDCC. Conversely, the anode powders were prepared by mixing nickel oxide (NiO) with 40 wt % SDCC via high-speed ball milling technique to obtain NiO–SDCC composite anodes [33].

The X-ray diffraction (XRD) patterns of the prepared LSCF–SDCC composite cathode powders were collected by using an X-ray diffractometer (Shimadzu XRD-6000, D8-Advance, Bruker, Germany) under the following conditions: CuKα (λ = 0.15418 nm) radiation, and 2θ varying from 10° to 80°. Energy-dispersive X-ray (EDX) spectroscopy was conducted to determine the elemental composition of the synthesized electrolyte, cathode, and anode powders, as shown in Figure 1. The EDX spectra confirmed the presence of Sm, Ce, La, Sr, Fe, Co, Ni, and Na peaks, detected from the synthesized powders. However, the Li peak cannot be detected easily by using a conventional EDX instrument, due to use of a beryllium filter. The cross-sectional microstructure of the fabricated single cells was observed through field emission scanning electron microscopy (FESEM, Merlin Compact, ZEISS, Germany). The specific surface area of the composite powders was determined using a BET surface area analyzer (Micrometritics, ASAP 2010, Norcross, Georgia USA). A laser particle sizer (Fritsch Analysette 22) was used to determine the particle size distribution of the prepared composite cathode powders.

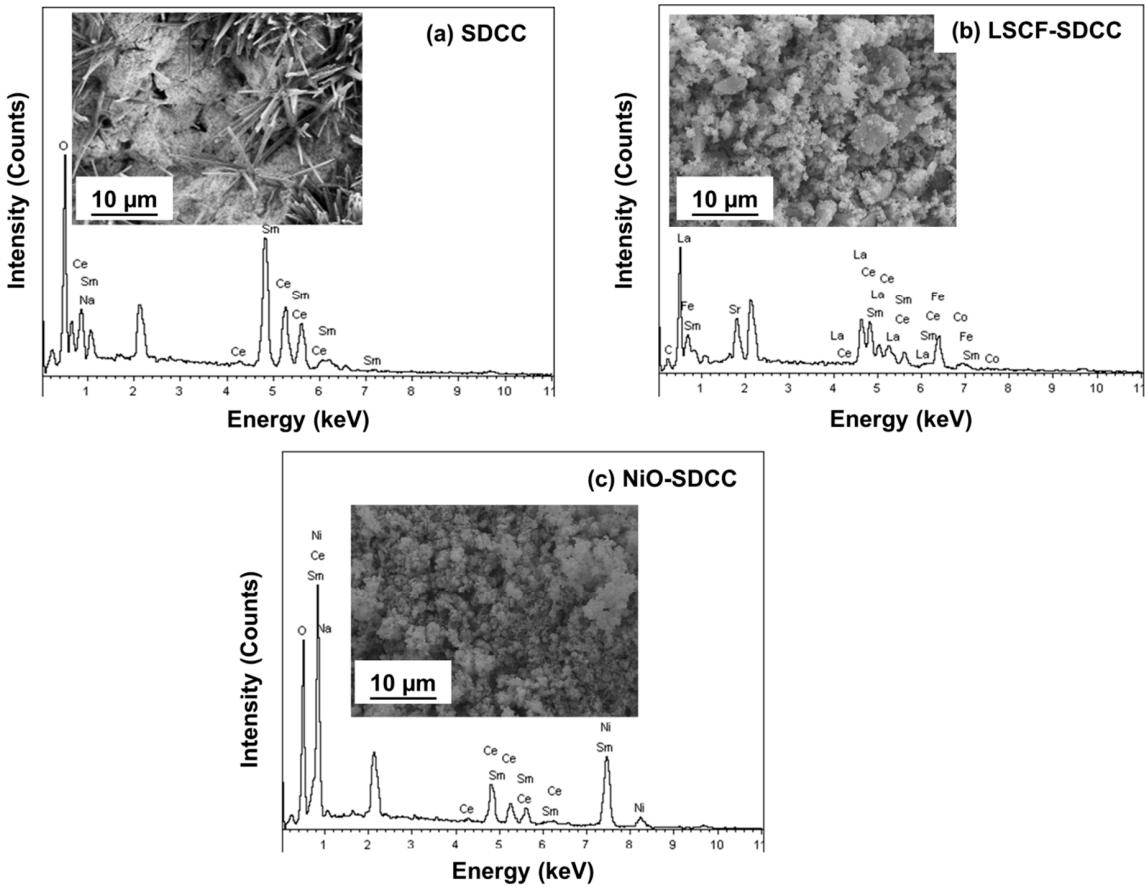

Figure 1. Energy-dispersive spectra and SEM images (insert) of (**a**) samarium doped ceria–carbonate (SDCC) electrolyte, (**b**) $La_{0.6}Sr_{0.4}Co_{0.2}Fe_{0.8}O_{3-\delta}$/samarium-doped ceria-carbonate (LSCF–SDCC) composite cathode, and (**c**) nickel oxide/ samarium-doped ceria-carbonate (NiO–SDCC) composite anode powders.

2.2. Electrochemical Characterization

The anode, electrolyte, and cathode were uniaxially pressed into a pellet (25 mm in diameter and 1.3 mm thickness) at a pressure of 200 MPa. The green pellet was co-sintered at 600 °C for 1 h in the air (Figure 2a). The thicknesses of the anode, electrolyte, and cathode layers were 0.5 mm, 0.5 mm, and 0.3 mm, respectively (Figure 2a). The effective working area of the pellets was 0.78 cm^2, and their cell structures are as follows:

NiO–SDCC|SDCC|LSCF–30SDCC	Cell A
NiO–SDCC|SDCC|LSCF–40SDCC	Cell B
NiO–SDCC|SDCC|LSCF–50SDCC	Cell C

The prepared single-button cells were tested by using a computerized SOFC test station (Chino, Japan). Current (*I*)-voltage (*V*) and power density (*P*) measurements performed at operating temperatures ranging from 500 °C to 650 °C using hydrogen and air were used as fuel and oxidant, respectively. The hydrogen flow rate was approximately 60 mL/min, and the air flow rate was maintained at 100 mL/min under 1 atm pressure.

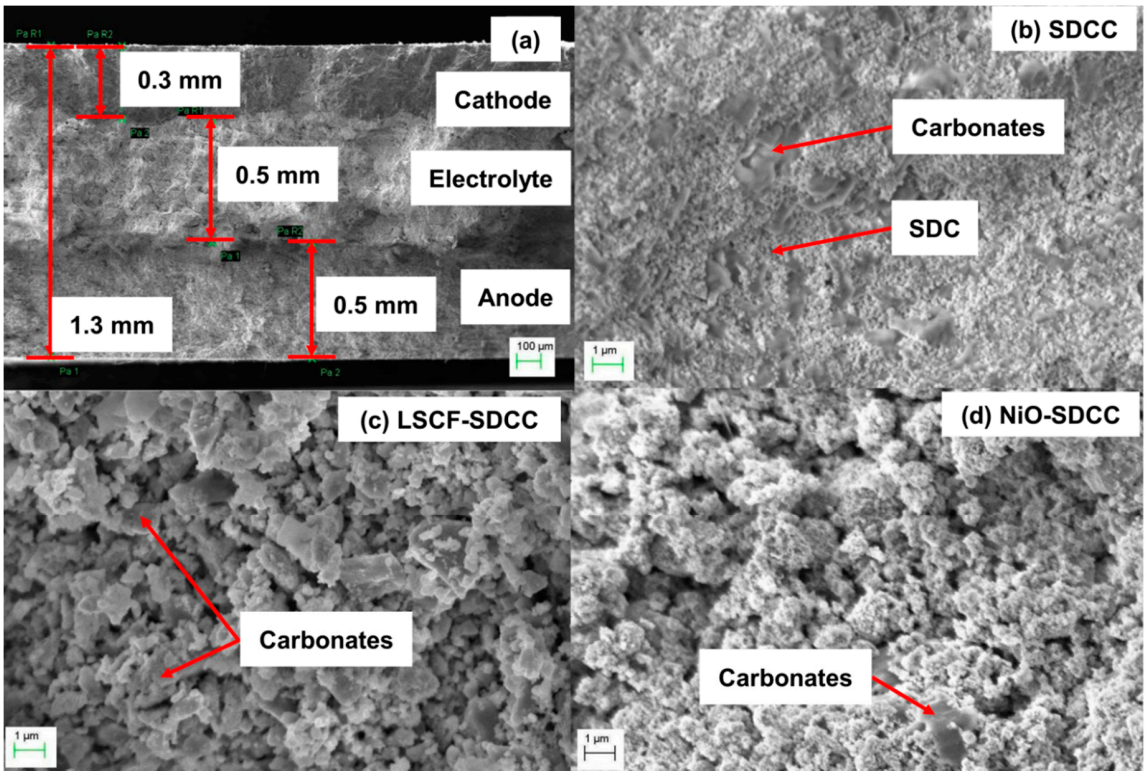

Figure 2. Cross-section FESEM images of (**a**) uniaxially pressed single-cell solid oxide fuel cell (SOFC), (**b**) SDCC composite electrolyte, (**c**) LSCF–SDCC composite cathode, and (**d**) NiO–SDCC composite anode.

3. Results and Discussion

3.1. Powder Characterizations

The XRD patterns of the LSCF–SDCC composite cathode with varying SDCC composite electrolyte contents are shown in Figure 3. The XRD pattern of the LSCF–SDCC composite cathode comprised LSCF and ceria peaks for all the samples and did not exhibit any phase change or formation of any secondary impurity phase upon mixing and calcination. The standard peaks of the perovskite-structured LSCF (space group R-3C [167], JPCDS PDF# 01-081-9113) and cubic fluorite SDC (space group Fm-3m [225], JPCDS PDF# 00-034-0394) were identified. The crystallite size (D_{XRD}) of the calcined powders were determined using the Scherrer equation [31]. Table 1 shows the D_{XRD} of the prepared composite cathode powders. The D_{XRD} values of the LSCF and SDCC starting powders were 31 and 63 nm, respectively. The XRD results show that the D_{XRD} of the LSCF–SDCC composite cathode increased. This increase indicates the occurrence of LSCF and SDCC crystallization during calcination at 680 °C for 1 h. However, the addition of SDCC composite electrolytes to the LSCF powders did not reveal any change in their phase structure, thus confirming the purity of the prepared LSCF–SDCC composite cathode powder [28]. However, the intensity of SDC diffraction peaks increased with SDCC composite electrolyte content, whereas that of the LSCF peaks decreased accordingly. This result can be considered as evidence of the increased SDCC nominal content in the composite cathode.

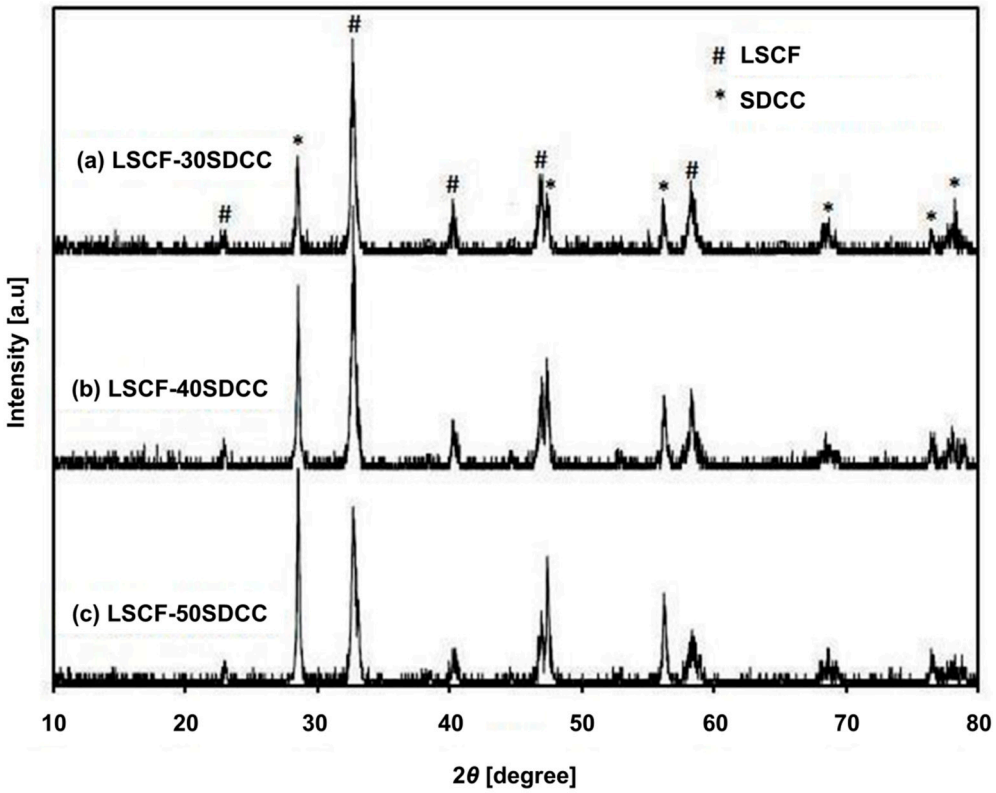

Figure 3. XRD patterns of LSCF–SDCC composite cathodes with different SDCC electrolyte contents: (**a**) LSCF–30SDCC, (**b**) LSCF–40SDCC, and (**c**) LSCF–50SDCC.

Table 1. Properties of the composite cathode LSCF–SDCC powders.

Samples	Surface Area (m^2/g)	Average Particle Size (nm)	Crystallite Size (nm)	
			LSCF	SDCC
LSCF–30SDCC	7.42	560	42	81
LSCF–40SDCC	4.39	642	49	102
LSCF–50SDCC	4.04	655	48	99

Specific surface area (S_{BET}) of the pure LSCF and SDCC powders were 11.8 and 4.24 m^2/g, respectively. A considerable difference was observed in the S_{BET} of the LSCF powders after mixing SDCC composite, due to increase in different powder particle size. In fact, the mean particle sizes of the pure LSCF and LSCF–50SDCC composite powders were 78 and 642 nm, respectively. This difference can be attributed to the presence of the macro-sized carbonates in the SDCC composite electrolyte and the formation of loose agglomerated particles upon synthesis and thermal treatment. The S_{BET} of the LSCF–SDCC composite cathode also gradually decreased with the increase in SDCC content. This result corresponded with the large particle size that resulted in small S_{BET} [34]. Table 1 shows that the average particle size of the LSCF–SDCC composite cathode gradually increased with the SDCC composite electrolyte content. Therefore, the SDCC composite electrolyte content influenced the S_{BET} and the particle size of the LSCF–SDCC composite cathode significantly more than the ball milling process and calcined temperature. The obtained S_{BET} of the LSCF–SDCC composite cathode is comparable with that in the literature [28].

3.2. Microstructure Characterization and Single Cell Performance

The cross-sectional microstructure of the single cell and its components are shown in Figure 2. Figure 2b shows dense morphology with no pores for the SDCC electrolyte layers, whereas the

anode and cathode layers exhibited loosely agglomerated and porous microstructures. The presence and distribution of the carbonate crystals in the microstructure were evident in all three layers. The carbonates formed a continuous network and homogenously dispersed on the SDC, LSCF, and NiO particles. However, identifying the individual constituent elements of LSCF, SDC, and NiO from the microstructure images of Figure 2c,d was difficult due to the presence of carbonate in the mixture and its melting characteristics.

The relationship between the SDCC composite electrolyte content and the properties of the LSCF–SDCC composite cathode was studied using *I–V* and *I–P* measurements in air and hydrogen. A schematic setup for single-cell electrochemical tests to measure the *I–V* and *I–P* characteristics of the single cell is shown in Figure 4. The carbonate-based fuel cells must be operated beyond the melting temperature of the carbonate, which is between 500 °C and 650 °C [35]. Therefore, the performances of the single button cells of cells A, B, and C were investigated between 500 °C to 650 °C, as shown in Figure 5a–c. The open-circuit voltage and power density of all the fabricated cells increased with temperature [36]. The influence of the LSCF–SDCC composite cathode composition on the single-cell performance was significant at different SDCC contents. The increase in SDCC composite electrolyte content in the LSCF cathode worsened the single-cell performance at all the operating temperatures. When the electrolyte content was below 40 wt %, cell A with 30 wt % SDCC composite electrolyte exhibited the highest performance, with a measured power density value of 75.4 mW/cm^2 at 650 °C. Therefore, the LSCF–SDCC composite cathode resistance can be reduced by using lower SDCC content (30 wt %) in the cathode microstructure. However, decreasing the SDCC content below 30 wt % could cause severe thermal expansion coefficient mismatch between the cathode and electrolyte components [29]. This could induce thermo-mechanical failure between the components during the operational conditions, thus causing cell failure.

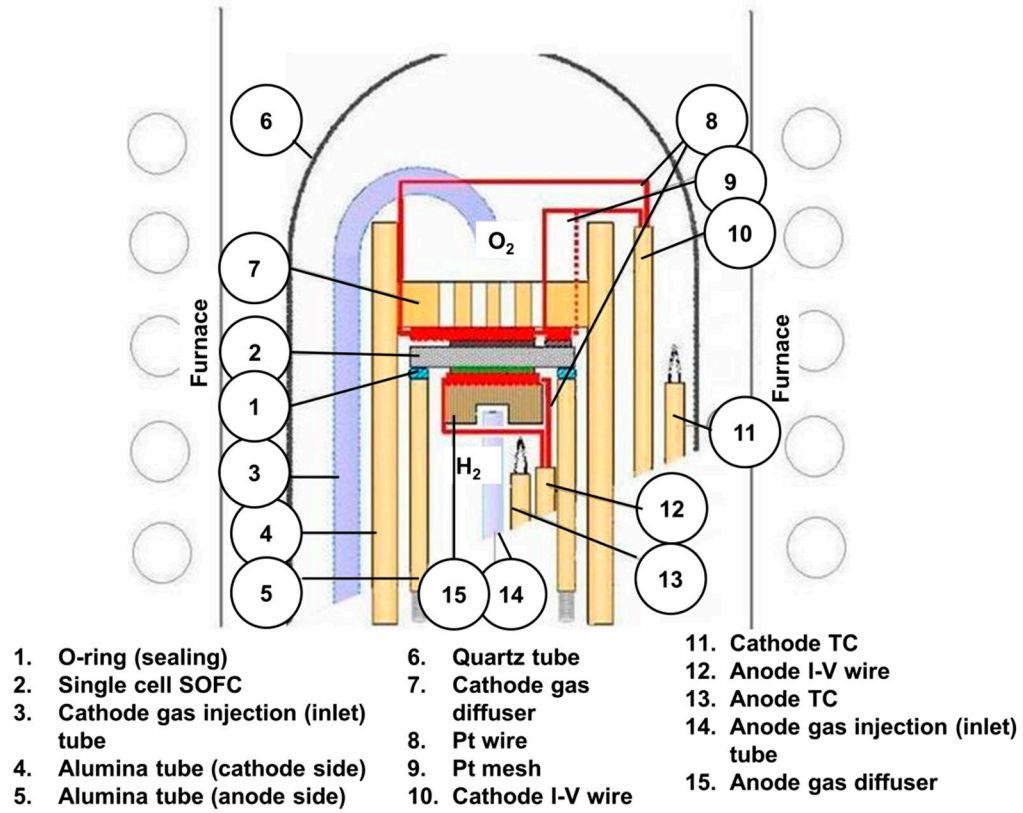

Figure 4. Schematic of the SOFC testing chamber.

The results obtained from this study were comparable with those of previous reports on single cells based on the LSCF composite cathode. For example, Zhang et al. reported a maximum density of 75 mW/cm^2 for a LSCF–SDC–Ag composite cathode-based fuel cell at the operating temperature of 650 °C [37]. In another study, Liu et al. obtained maximum power densities of 35 and 60 mW/cm^2 at 550 °C and 600 °C, respectively [38]. However, the power density values obtained here were significantly lower than those earlier reported in the literature on the single cell based on SDCC composite electrolytes, as shown in Table 2. This difference in performance of the single cell based on SDCC composite electrolytes can be ascribed to the choice of electrode materials and carbonates and their compositions and fabrication conditions. Therefore, the SOFC single-cell performance can be improved by optimizing the physical properties and microstructure of the cell components. Developing high performance materials and adopting cost-effective fabrication techniques to produce thin films can improve the performance of low temperature solid oxide fuel cells (LT–SOFC) [39].

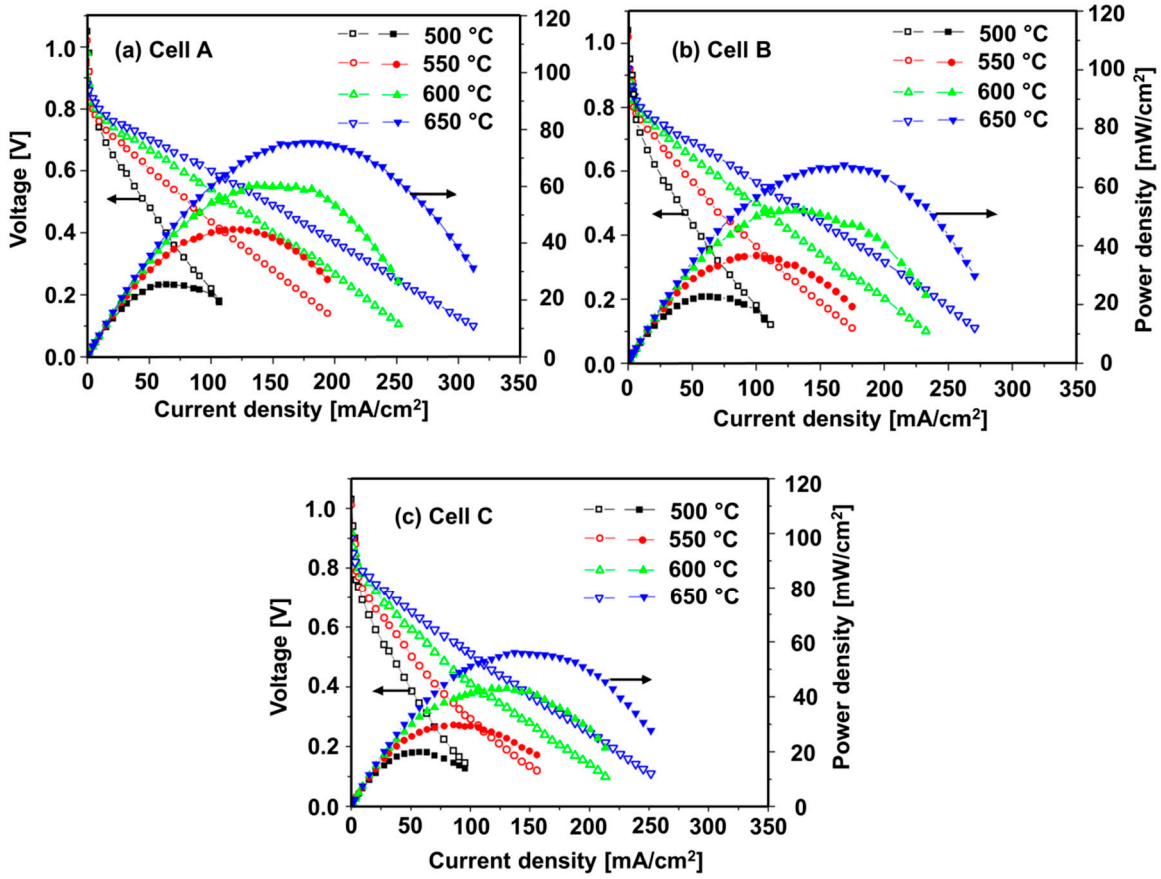

Figure 5. Performance of single cell at 500 °C, 550 °C, 600 °C, and 650 °C: (**a**) cells A, (**b**) B, and (**c**) C.

Table 2. Comparison of single-cell performance based on doped ceria–carbonate composite electrolyte materials.

Electrolyte	Cathode	Anode	Fuel (Anode/Cathode)	Current Collecting Layer	Operating Temperature (°C)	Power Density (mW/cm^2)	Reference
SDC–30 wt % $Li1.34Na0.66CO_3$	LSCF–30 wt % SDC–$Li1.34Na0.66CO_3$	NiO–40 wt % SDC–$Li1.34Na0.66CO_3$	H_2/air	-	650	75.4	This study
SDC–20 wt % $(LiNa)_2CO_3$	lithiated NiO-SDC–$(LiNa)_2CO_3$	NiO–SDC–$(LiNa)_2CO_3$	H_2/O_2	-	575	600	[8]
SDC–20 wt % $(LiNa)_2CO_3$	LSCF–50 wt % SDC–$(LiNa)_2CO_3$	NiO–50 wt % SDC–$(LiNa)_2CO_3$	H_2/O_2	Silver	550	120.4	[28]
SDC–35 wt % $(LiNaK)_2CO_3$	LSCF–45 wt % SDC–$(LiNaK)_2CO_3$	NiO–45 wt % SDC–$(LiNaK)_2CO_3$	$H_2/O_2 + CO_2$	-	550	801	[40]
SDC–46.8 wt % Na_2CO_3	lithiated NiO–60 wt % SDC–Na_2CO_3	NiO–60 wt % SDC–Na_2CO_3	H_2/air	Silver	550	342	[41]
SDC–$(LiNa)_2CO_3$	LiNiCuZnO	LiNiCuZnO–SDCC	H_2/air	-	600	617	[26]
SDC–$(LiNa)_2CO_3$	LiNiCuZnO–SDCC	LiNiCuZnO–SDCC	H_2/O_2	Silver	580	520	[42]

Under fuel cell conditions, multi-conduction paths or mobility of various ions from the constituent phases (such as Li^+, Na^+, K^+, H^+, CO_3^{2-}, and O^{2-}) co-exist inside the composite electrolyte materials [43]. This mixed-ionic property of carbonate-based electrolyte materials leads to superionic conduction behavior, thus exhibiting superior ionic conductivity at low operating temperatures. Moreover, the presence of the molten carbonate phase in the electrode microstructure could minimize the electrolyte–electrode interface polarization resistance, by enlarging the triple-phase boundary [44]. This condition contributes toward the fast ion transport of O^{2-} and H^+ ions at the electrolyte–electrode interface, consequently increasing the overall cell performance [45]. The presence of a molten carbonate enhances the oxygen adsorption (Equations (1)–(3)) and promotes the oxygen reduction reaction process (Equation (4)) with the formation of intermediate products (CO_4^{2-} and CO_5^{2-}) from CO_3^{2-} and O_2 [46].

$$CO_3^{2-} + O_2 \leftrightarrow CO_5^{2-} \quad (1)$$

$$CO_5^{2-} + CO_3^{2-} \leftrightarrow 2CO_4^{2-} \quad (2)$$

$$2CO_3^{2-} + O_2 \leftrightarrow 2CO_4^{2-} \quad (3)$$

$$CO_4^{2-} + 2e^- \leftrightarrow CO_3^{2-} + O^{2-} \quad (4)$$

However, incorporating this mixed multi-ionic conducting SDCC composite electrolyte to electrode materials could eventually suppress the electronic conduction behavior of the LSCF cathode materials and thereby deteriorate the oxygen reduction reaction (ORR) kinetics at the surface [47]. This condition is attributable to the carbonates because they do not conduct or prevent electrons from moving from one ceria particle to another [45]. Moreover, carbonates are generally added to the doped ceria electrolytes to avoid localized electron conduction in ceria at temperatures above 600 °C. The electronic conduction contribution in ceria is due to the partial reduction of Ce^{4+} to Ce^{3+} in reducing environment, which decreases the overall cell efficiency and contributes to enhancing mechanical stability issues [26,48]. Dissociation/ionization of adsorbed oxygen molecules required electrons to diffuse oxygen (O^{2-}) ions through the bulk of the cathode microstructure and the interface region. This reaction can be expressed by using the Kroger–Vink notation:

$$1/2O_2 + 2e^- + V_O^{\cdot\cdot} \rightarrow O_O^{\times} \quad (5)$$

When hydrogen and air are used as fuel, H^+/O^{2-} ion conduction occurs in the carbonate-based fuel cells, leading to superior cell performance. The possible ion electrode reaction mechanism at the cathode side can be expressed as follows [49]:

H^+ ion conduction at the cathode side:

$$1/2O_2 + 2H^+ + 2e^- \rightarrow H_2O^{2^-}. \quad (6)$$

Ion conduction at the cathode side:

$$1/2O_2 + 2e^- \rightarrow O^{2-}. \quad (7)$$

Reactions (6) and (7) show that the ORR reaction requires electrons (e^-) for the ionization of adsorbed oxygen molecules, and ORR kinetics are associated with the number of oxygen molecules adsorbed on the LSCF surface [50]. The composite cathode microstructure (Figure 2c) reveals that the particle connectivity among LSCF particles was poor due to the presence of molten carbonate and SDC particles. This finding could considerably affect the electronic network over the LSCF surface, consequently blocking the conduction paths between the LSCF and SDCC particles, and decreasing the single-cell performance [20]. The results of our study proved that the single-cell performance decreased with increased SDCC composite electrolyte content. Therefore, this finding suggests that the formation of O^{2-} ions at the surface of the composite cathode probably affected the ORR rate [16].

Shah et al. also reported a similar finding for LSCF-based composite materials [51]. However, in-plane electronic conductivity for the rapid formation of O^{2-} ions by electron conduction can be enhanced by printing or depositing a thin current-collecting layer (CCL) on the LSCF–SDCC composite cathode surface [52]. As shown in Table 2, Ag was used as a CCL on the electrode surface to improve the in-plane electronic conductivity and achieve high performance at low operating temperatures. For instance, Rahman et al. reported a higher power density value of 120.4 mW/cm^2 at 750 °C for a single cell fabricated with LSCF–50 wt % SDCC composite cathode by using Ag as CCL [28]. This shows that the presence of CCL could help to minimize the rate-limiting factor associated with the surface exchange reaction, and the formation and diffusion of H^+/O^{2-} ions at the composite cathode side. Therefore, adding SDC–carbonate composite electrolyte materials to the LSCF cathode system could considerably influence the performance of the single LT–SOFC cell with the presence of a thin CCL layer on the surface of the cathode functional layer.

4. Conclusions

The effect of different SDCC composite electrolyte contents (30, 40, and 50 wt %) on the phase structure, microstructure, specific surface area, and electrochemical performance of the LSCF–SDCC composite cathodes were investigated in view of a possible real application for LT–SOFCs. The electrochemical performance showed that the composite cathode with 30 wt % SDCC exhibited the highest value of power density equal to 75.4 mW/cm^2 at 650 °C. Increasing the amount of the SDCC content in the composite cathode decreased the overall performance due to poor in-plane electronic conduction at the surface of the LSCF cathode layer. The FESEM results revealed that the LSCF particles were covered with the SDC and molten carbonate phase. This condition limited the LSCF particle-to-particle connectivity, decreasing the overall performance of the single cell for increasing contents of SDCC composite electrolyte. Therefore, the ionization of the adsorbed oxygen at the surface of the LSCF cathode was hindered, thus leading to a significant performance degradation of the LT–SOFC cathode.

Author Contributions: Writing-original draft preparation, data curation, methodology, M.A.S.A.; Conceptualization, methodology, J.R.; Conceptualization, Writing–review and editing, D.S.K.; M.A. and L.S.; Writing–review and editing, Project administration, funding acquisition, supervision, A.M.; Resources, M.R.S. All authors have read and agreed to the published version of the manuscript.

Funding: This research received no external funding.

Acknowledgments: This work was supported by the Universiti Kebangsaan Malaysia (UKM) and the Ministry of Education, Malaysia through the postdoctoral research grant no. MI-2019-019. The authors would also like to thank the Center for Research and Instrumentation Management of UKM for allowing the use of their excellent testing equipment.

Conflicts of Interest: The authors declare no conflict of interest.

References

1. Wan Yusof, W.N.A.; Abdul Samat, A.; Norman, N.W.; Somalu, M.R.; Muchtar, A.; Baharuddin, N.A. Synthesis and Characterization of Zn-doped $LiCoO_2$ Material Prepared via Glycinenitrate Combustion Method for Proton Conducting Solid Oxide Fuel Cell Application. *J. Kejuruter.* **2018**, *SI1*, 11–15.
2. Shaikh, S.P.S.; Muchtar, A.; Somalu, M.R. A review on the selection of anode materials for solid-oxide fuel cells. *Renew. Sustain. Energy Rev.* **2015**, *51*, 1–8. [CrossRef]
3. Cebollero, J.A.; Lahoz, R.; Laguna-Bercero, M.A.; Larrea, A. Tailoring the electrode-electrolyte interface of Solid Oxide Fuel Cells (SOFC) by laser micro-patterning to improve their electrochemical performance. *J. Power Sources* **2017**, *360*, 336–344. [CrossRef]
4. Javed, H.; Sabato, A.G.; Herbrig, K.; Ferrero, D.; Walter, C.; Salvo, M.; Smeacetto, F. Design and characterization of novel glass-ceramic sealants for solid oxide electrolysis cell (SOEC) applications. *Int. J. Appl. Ceram. Technol.* **2018**, *15*, 999–1010. [CrossRef]

5. Elsayed, H.; Javed, H.; Sabato, A.G.; Smeacetto, F.; Bernardo, E. Novel glass-ceramic SOFC sealants from glass powders and a reactive silicone binder. *J. Eur. Ceram. Soc.* **2018**, *38*, 4245–4251. [CrossRef]
6. Slim, C.; Baklouti, L.; Cassir, M.; Ringuedé, A. Structural and electrochemical performance of gadolinia-doped ceria mixed with alkali chlorides (LiCl-KCl) for Intermediate Temperature-Hybrid Fuel Cell applications. *Electrochim. Acta* **2014**, *123*, 127–134. [CrossRef]
7. Dong, X.; Tian, L.; Li, J.; Zhao, Y.; Tian, Y.; Li, Y. Single layer fuel cell based on a composite of $Ce_{0.8}Sm_{0.2}O_{2-\delta}$-$Na_2CO_3$ and a mixed ionic and electronic conductor $Sr_2Fe_{1.5}Mo_{.5}O_{6-\delta}$. *J. Power Sources* **2014**, *249*, 270–276. [CrossRef]
8. Chen, M.; Zhang, H.; Fan, L.; Wang, C.; Zhu, B. Ceria-carbonate composite for low temperature solid oxide fuel cell: Sintering aid and composite effect. *Int. J. Hydrog. Energy* **2014**, *39*, 12309–12316. [CrossRef]
9. Zhang, L.; Lan, R.; Tao, S. An intermediate temperature fuel cell based on composite electrolyte of carbonate and doped barium cerate with $SrFe_{0.7}Mn_{0.2}Mo_{0.1}O_{3-\delta}$ cathode. *Int. J. Hydrog. Energy* **2013**, *38*, 16546–16551. [CrossRef]
10. Mat, M.D.; Liu, X.; Zhu, Z.; Zhu, B. Development of cathodes for methanol and ethanol fuelled low temperature (300-600 °C) solid oxide fuel cells. *Int. J. Hydrog. Energy* **2007**, *32*, 796–801. [CrossRef]
11. Zhu, B.; Fan, L.; Lund, P. Breakthrough fuel cell technology using ceria-based multi-functional nanocomposites. *Appl. Energy* **2013**, *106*, 163–175. [CrossRef]
12. Mostafavi, E.; Babaei, A.; Ataie, A. $La_{0.6}Sr_{0.4}Co_{0.2}Fe_{0.8}O_3$ perovskite cathode for intermediate temperature solid oxide fuel cells: A comparative study. *Iran. J. Hydrog. Fuel Cell* **2014**, *4*, 239–246.
13. Shimura, K.; Nishino, H.; Kakinuma, K.; Brito, M.E.; Uchida, H. Effect of samaria-doped ceria (SDC) interlayer on the performance of $La_{0.6}Sr_{0.4}Co_{0.2}Fe_{0.8}O_{3-\delta}$/SDC composite oxygen electrode for reversible solid oxide fuel cells. *Electrochim. Acta* **2017**, *225*, 114–120. [CrossRef]
14. Spiridigliozzi, L.; Dell'Agli, G.; Accardo, G.; Yoon, S.P.; Frattini, D. Electro-morphological, structural, thermal and ionic conduction properties of Gd/Pr co-doped ceria electrolytes exhibiting mixed Pr3+/Pr4+ cations. *Ceram. Int.* **2019**, *45*, 4570–4580. [CrossRef]
15. Spiridigliozzi, L. *Doped-Ceria Electrolytes: Synthesis, Sintering and Characterization*; SpringerBriefs in Applied Sciences and Technology; Springer International Publishing: Cham, Switzerland, 2018; ISBN 978-3-319-99394-2.
16. Jaiswal, N.; Tanwar, K.; Suman, R.; Kumar, D.; Uppadhya, S.; Parkash, O. A brief review on ceria based solid electrolytes for solid oxide fuel cells. *J. Alloys Compd.* **2019**, *781*, 984–1005. [CrossRef]
17. Liu, Y.; Chen, K.; Zhao, L.; Chi, B.; Pu, J. Performance stability and degradation mechanism of $La_{0.6}Sr_{0.4}Co_{0.2}Fe_{0.8}O_{3-\delta}$ cathodes under solid oxide fuel cells operation conditions. *Int. J. Hydrog. Energy* **2014**, *39*, 15868–15876. [CrossRef]
18. Fan, E.S.C.; Kuhn, J.; Kesler, O. Suspension plasma spraying of $La_{0.6}Sr_{0.4}Co_{0.2}Fe_{0.8}O_{3-\delta}$ cathodes: Influence of carbon black pore former on performance and degradation. *J. Power Sources* **2016**, *316*, 72–84. [CrossRef]
19. Yan, D.; Zhang, C.; Liang, L.; Li, K.; Jia, L.; Pu, J.; Jian, L.; Li, X.; Zhang, T. Degradation analysis and durability improvement for SOFC 1-cell stack. *Appl. Energy* **2016**, *175*, 414–420. [CrossRef]
20. Furukawa, N.; Sameshima, S.; Hirata, Y.; Shimonosono, T. Influence of cathode on electric power of solid oxide fuel cells. *J. Ceram. Soc. Jpn.* **2014**, *122*, 226–229. [CrossRef]
21. Mosiaek, M.; Kdra, A.; Krzan, M.; Bielaska, E.; Tatko, M. $Ba_{0.5}Sr_{0.5}Co_{0.8}Fe_{0.2}O_3$-$La_{0.6}Sr_{0.4}Co_{0.8}Fe_{0.2}O_3$-composite cathode for solid oxide fuel cell. *Arch. Metall. Mater.* **2016**, *61*, 1137–1142. [CrossRef]
22. Jaiswal, N.; Upadhyay, S.; Kumar, D.; Parkash, O. Enhanced ionic conductivity in La^{3+} and Sr^{2+} co-doped ceria: Carbonate nanocomposite. *Ionics* **2015**, *21*, 2277–2283. [CrossRef]
23. Raza, R.; Wang, X.; Ma, Y.; Liu, X.; Zhu, B. Improved ceria-carbonate composite electrolytes. *Int. J. Hydrog. Energy* **2010**, *35*, 2684–2688. [CrossRef]
24. Fan, L.; Wang, C.; Chen, M.; Zhu, B. Recent development of ceria-based (nano)composite materials for low temperature ceramic fuel cells and electrolyte-free fuel cells. *J. Power Sources* **2013**, *234*, 154–174. [CrossRef]
25. Ristoiu, T.; Petrisor, T.; Gabor, M.; Rada, S.; Popa, F.; Ciontea, L.; Petrisor, T. Electrical properties of ceria/carbonate nanocomposites. *J. Alloys Compd.* **2012**, *532*, 109–113. [CrossRef]
26. Ali, A.; Rafique, A.; Kaleemullah, M.; Abbas, G.; Ajmal Khan, M.; Ahmad, M.A.; Raza, R. Effect of Alkali Carbonates (Single, Binary, and Ternary) on Doped Ceria: A Composite Electrolyte for Low-Temperature Solid Oxide Fuel Cells. *ACS Appl. Mater. Interfaces* **2018**, *10*, 806–818. [CrossRef]

27. Huang, J.; Mao, Z.; Liu, Z.; Wang, C. Performance of fuel cells with proton-conducting ceria-based composite electrolyte and nickel-based electrodes. *J. Power Sources* **2008**, *175*, 238–243. [CrossRef]
28. Rahman, H.A.; Muchtar, A.; Muhamad, N.; Abdullah, H. $La_{0.6}Sr_{0.4}Co_{0.2}Fe_{0.8}O_{3-\delta}$-SDC carbonate composite cathodes for low-temperature solid oxide fuel cells. *Mater. Chem. Phys.* **2013**, *141*, 752–757. [CrossRef]
29. Rahman, H.A.; Muchtar, A.; Muhamad, N.; Abdullah, H. Structure and thermal properties of $La_{0.6}Sr_{0.4}Co_{0.2}Fe_{0.8}O_{3-\delta}$-SDC carbonate composite cathodes for intermediate- to low-temperature solid oxide fuel cells. *Ceram. Int.* **2012**, *38*, 1571–1576. [CrossRef]
30. Muhammed Ali, S.A.; Anwar, M.; Ashikin, N.; Muchtar, A.; Somalu, M.R. Influence of oxygen ion enrichment on optical, mechanical, and electrical properties of LSCF perovskite nanocomposite. *Ceram. Int.* **2018**, *44*, 10433–10442. [CrossRef]
31. Muhammed Ali, S.A.; Muchtar, A.; Bakar Sulong, A.; Muhamad, N.; Herianto Majlan, E. Influence of sintering temperature on the power density of samarium-doped-ceria carbonate electrolyte composites for low-temperature solid oxide fuel cells. *Ceram. Int.* **2013**, *39*, 5813–5820. [CrossRef]
32. Muhammed Ali, S.A.; Rosli, R.E.; Muchtar, A.; Sulong, A.B.; Somalu, M.R.; Majlan, E.H. Effect of sintering temperature on surface morphology and electrical properties of samarium-doped ceria carbonate for solid oxide fuel cells. *Ceram. Int.* **2015**, *41*, 1323–1332. [CrossRef]
33. Jarot, R.; Muchtar, A.; Wan Daud, W.R.; Muhamad, N.; Majlan, E.H. Porous NiO-SDC carbonates composite anode for LT-SOFC applications produced by pressureless sintering. *Appl. Mech. Mater.* **2011**, *52*, 488–493. [CrossRef]
34. Zhang, J.; Huang, X.; Zhang, H.; Xue, Q.; Xu, H.; Wang, L.; Feng, Z. The effect of powder grain size on the microstructure and electrical properties of 8 mol% Y_2O_3-stabilized ZrO_2. *RSC Adv.* **2017**, *7*, 39153–39159. [CrossRef]
35. Liu, W.; Liu, Y.; Li, B.; Sparks, T.D.; Wei, X.; Pan, W. Ceria (Sm^{3+}, Nd^{3+})/carbonates composite electrolytes with high electrical conductivity at low temperature. *Compos. Sci. Technol.* **2010**, *70*, 181–185. [CrossRef]
36. Kosinski, M.R.; Baker, R.T. Preparation and property-performance relationships in samarium-doped ceria nanopowders for solid oxide fuel cell electrolytes. *J. Power Sources* **2011**, *196*, 2498–2512. [CrossRef]
37. Zhang, J.; Ji, Y.; Gao, H.; He, T.; Liu, J. Composite cathode $La_{0.6}Sr_{0.4}Co_{0.2}Fe_{0.8}O_3$-$Sm_{0.1}Ce_{0.9}O_{1.95}$-Ag for intermediate-temperature solid oxide fuel cells. *J. Alloys Compd.* **2005**, *395*, 322–325. [CrossRef]
38. Liu, Y.; Hashimoto, S.; Nishino, H.; Takei, K.; Mori, M. Fabrication and characterization of a co-fired $La_{0.6}Sr_{0.4}Co_{0.2}Fe_{0.8}O_{3-\delta}$ cathode-supported $Ce_{0.9}Gd_{0.1}O_{1.95}$ thin-film for IT-SOFCs. *J. Power Sources* **2007**, *164*, 56–64. [CrossRef]
39. Rondão, A.I.B.; Patrício, S.G.; Figueiredo, F.M.L.; Marques, F.M.B. Composite electrolytes for fuel cells: Long-term stability under variable atmosphere. *Int. J. Hydrog. Energy* **2014**, *39*, 5460–5469. [CrossRef]
40. Khan, I.; Asghar, M.I.; Lund, P.D.; Basu, S. High conductive $(LiNaK)_2CO_3$–$Ce_{0.85}Sm_{0.15}O_2$ electrolyte compositions for IT-SOFC applications. *Int. J. Hydrog. Energy* **2017**, *42*, 20904–20909. [CrossRef]
41. Li, C.; Zeng, Y.; Wang, Z.; Ye, Z.; Zhang, Y.; Shi, R. Preparation of SDC-NC nanocomposite electrolytes with elevated densities: Influence of prefiring and sintering treatments on their microstructures and electrical conductivities. *RSC Adv.* **2016**, *6*, 99615–99624. [CrossRef]
42. Irshad, M.; Siraj, K.; Raza, R.; Javed, F.; Ahsan, M.; Shakir, I.; Rafique, M.S. High performance of SDC and GDC core shell type composite electrolytes using methane as a fuel for low temperature SOFC. *AIP Adv.* **2016**, *6*, 025202. [CrossRef]
43. Anwar, M.; Muhammed Ali, S.A.; Muchtar, A.; Somalu, M.R. Synthesis and characterization of M-doped ceria-ternary carbonate composite electrolytes (M=erbium, lanthanum and strontium) for low-temperature solid oxide fuel cells. *J. Alloys Compd.* **2019**, *775*, 571–580. [CrossRef]
44. Fan, L.; He, C.; Zhu, B. Role of carbonate phase in ceria-carbonate composite for low temperature solid oxide fuel cells: A review. *Int. J. Energy Res.* **2017**, *41*, 465–481. [CrossRef]
45. Raza, R.; Zhu, B.; Rafique, A.; Naqvi, M.R.; Lund, P. Functional ceria-based nanocomposites for advanced low-temperature (300–600 °C) solid oxide fuel cell: A comprehensive review. *Mater. Today Energy* **2020**, *15*, 100373. [CrossRef]
46. Qin, C.; Gladney, A. DFT study of CO_4^{2-} and CO_5^{2-} relevant to oxygen reduction with the presence of molten carbonate in solid oxide fuel cells. *Comput. Theor. Chem.* **2012**, *999*, 179–183. [CrossRef]

47. Muhammed Ali, S.A.; Anwar, M.; Mahmud, L.S.; Kalib, N.S.; Muchtar, A.; Somalu, M.R. Influence of current collecting and functional layer thickness on the performance stability of $La_{0.6}Sr_{0.4}Co_{0.2}Fe_{0.8}O_{3-\delta}$-$Ce_{0.8}Sm_{0.2}O_{1.9}$ composite cathode. *J. Solid State Electrochem.* **2019**, *23*, 1155–1164. [CrossRef]
48. Dell'Agli, G.; Spiridigliozzi, L.; Pansini, M.; Accardo, G.; Yoon, S.P.; Frattini, D. Effect of the carbonate environment on morphology and sintering behaviour of variously co-doped (Ca, Sr, Er, Pr) Samarium-doped Ceria in co-precipitation/hydrothermal synthesis. *Ceram. Int.* **2018**, *44*, 17935–17944. [CrossRef]
49. Zhao, Y.; Xia, C.; Xu, Z.; Li, Y. Validation of H^+/O^{2-} conduction in doped ceria-carbonate composite material using an electrochemical pumping method. *Int. J. Hydrog. Energy* **2012**, *37*, 11378–11382. [CrossRef]
50. Baek, S.W.; Bae, J.; Kim, J.H. Oxygen reduction mechanism at Sm0.5Sr0.5CoO3-δ/Sm0.2Ce0.8O1.9 composite cathode for solid oxide fuel cell. In Proceedings of the FUELCELL2008, 6th International Conference on Fuel Cell Science, Engineering and Technology, Denver, CO, USA, 16–18 July 2008; pp. 1–4.
51. Shah, M.; Barnett, S.A. Solid oxide fuel cell cathodes by infiltration of $La_{0.6}Sr_{0.4}Co_{0.2}Fe_{0.8}O_{3-\delta}$ into Gd-Doped Ceria. *Solid State Ionics* **2008**, *179*, 2059–2064. [CrossRef]
52. Sar, J.; Dessemond, L.; Djurado, E. Electrochemical properties of graded and homogeneous $Ce_{0.9}Gd_{0.1}O_{2-\delta}$–$La_{0.6}Sr_{0.4}Co_{0.2}Fe_{0.8}O_{3-\delta}$ composite electrodes for intermediate-temperature solid oxide fuel cells. *Int. J. Hydrog. Energy* **2016**, *41*, 17037–17043. [CrossRef]